Scanning Microscopy

Volume 5 | Number 2 Article 6

5-12-1991

Error Voltage Components in Quantitative Voltage Contrast Measurement Systems

D. S. H. Chan
National University of Singapore

T. S. Low
National University of Singapore

J. C. H. Phang
National University of Singapore

Scanning Microscopy, Vol. 5, No. 2, 1991 (Pages 345-355)
Scanning Microscopy International, Chicago (AMF O'Hare), IL 60666 USA

0891-7035/91$3.00+.00

ERROR VOLTAGE COMPONENTS IN QUANTITATIVE VOLTAGE CONTRAST MEASUREMENT SYSTEMS

DSH Chan*, TS Low, WK Chim and JCH Phang

Electrical Engineering Department, National University of Singapore,
10 Kent Ridge Crescent, Singapore 0511.

(Received for publication August 4, 1990, and in revised form May 12, 1991)

Abstract

This paper presents the results of computer simulation studies into the respective contributions of the potential barrier, the off-normal incidence injection of secondary electrons (SEs) into the retarding field and analyser geometry on Types I and II local field error voltages for a practical 20 mm wide planar retarding field energy analyser. Results show that the error voltage component due to the off-normal incidence injection effect of SEs into the retarding field dominates the Type I local field error. For type II LFE, the error voltage component due to analyser geometry effect is the higher contributing factor. The presence of a neighbouring electrode voltage tends to draw SEs away from the central axis of the energy analyser, thus causing the electron trajectories to be more sensitive to the influence of the analyser geometry.

KEY WORDS: Quantitative voltage contrast measurements, computer simulation, potential barrier, off-normal incidence injection, analyser geometry, secondary electrons, retarding field, types I and II local field effects, energy analyser, electron trajectories.

*Address for correspondence:
DSH Chan, Electrical Engineering Department, National University of Singapore, 10 Kent Ridge Crescent, Singapore 0511. (Tel: 772-2117)

Introduction

The voltage contrast effect in the scanning electron microscope (SEM) was first reported in 1957 by Oatley and Everhart [13]. This technique has now become a powerful tool for qualitative voltage imaging and for failure analysis of integrated circuits (ICs) [14]. Compared to the conventional mechanical probe, this technique offers higher spatial and temporal resolutions with virtually no loading effect and damage to the circuit under test. In recent years, the quantitative version of this technique has become important due to the increased density of VLSI chips and the reduced dimensions of conductor tracks. A number of electron beam testing systems or SEMs equipped with voltage contrast options has been introduced recently.

Although the application of the voltage contrast technique in the semiconductor industry is widely accepted, its full potential in the quantitative testing of ICs has not been realised. This is because the accuracy is currently limited by the presence of local fields above the conductor track being measured and by the effect of voltages on adjacent conductor tracks. These effects are known as type I and type II local field effects respectively and have come under extensive investigations [10,6,12,4,3,8,5]. There is presently insufficient quantitative data on the various factors which give rise to the error voltages. Most studies on quantitative voltage contrast have measured or simulated the total error voltage for a particular energy analyser-specimen configuration. The mechanisms that give rise to the total error voltage are (a) the potential barrier effect, (b) the off-normal incidence injection of secondary electrons (SEs) into the retarding field, (c) the analyser geometry effect and (d) the lens effect of the analyser grids. The contribution of each of these mechanisms to the total error voltage have not been reported. This information is necessary for a systematic approach to the design of low error voltage energy analysers as it provides an understanding of the major contributors to the error voltage in quantitative voltage contrast detectors. This paper presents the results of computer simulation studies which isolate the various error voltage components in quantitative voltage contrast measurements. The use of a planar analyser with electrostatic extraction and retarding fields is assumed.

When a conductor track with finite width is biased at a certain voltage, a potential barrier is set up. This barrier

filters out the low energy SEs and thus introduces non-linearities to potential measurements, especially if the feedback approach is used [6,12].

The off-normal incidence injection effect is due to the SE trajectories not being perfectly normal to the extraction grid plane as the SEs passes through the latter into the retarding or analysing field. This results from the angular distribution of emitted SEs and the modification of SE trajectories when they pass through non-uniform fields between the specimen and the extraction grid. A 5 V retarding barrier, for example, will thus not act as a perfect high pass filter with a sharp cut-off at 5 eV. As a result, SEs with energies greater than 5 eV and emitted at oblique incidence could be rejected by the retarding field. This introduces non-linearities and errors to the voltage measurement in planar retarding field analysers [6,12,4].

The third error voltage component, associated with the analyser geometry effect, is due to the finite width of the analyser acting as a stop to high energy SEs which have been emitted at oblique angles of incidence [1]. These SEs might otherwise have been able to overcome the potential barrier and retarding field and been collected if the analyser had been infinitely wide. This error component has been reported in narrow analysers and in situations where the voltage measurement point on the specimen is very close to the edge of the analyser [1]. The results for analyser geometry effect presented in this study are for a much wider energy analyser.

The lens effect is a result of the non-uniform potential distribution across the surface of the analyser grids. This effect will contribute to an extra error voltage component as the resulting lateral fields will alter the SE trajectories as they travel between the specimen and the retarding grid. This effect is expected to be particularly strong when high extraction voltages are used. This effect is still currently under investigation and the magnitude of this effect will be reported separately at a later date.

Computer Simulation Model

Physical Description of Model

Two two-dimensional models were used for studying the various error components on SEM voltage contrast. The larger model is shown in fig. 1. A planar retarding grid analyser is placed above the specimen. The specimen consists of three electrodes - the electrode being probed and two neighbouring electrodes whose voltages are denoted by VS, V1 and V2 respectively. The electrode dimensions, a, and inter-electrode spacing, b, are both 5 μms. In the model, the analyser grid meshes are assumed to be fine enough for the extraction and retarding grids to be represented as equipotential surfaces. In such a situation, the lens effect or the effect of the non-uniform field distribution across the surface of the analyser grids will be absent.

The width of the analyser used in the simulation was chosen to be 20 mm, which is close to the width commonly found in energy analysers. As shown in fig. 1, the heights above the specimen plane of the extraction grid, retarding grid and the reflection grid are respectively 2 mm, 6 mm and 31 mm. The entire simulation model, of dimensions 20 mm by 31 mm, is divided into 95 points along the horizontal axis and 60 points along the vertical axis. This results in 5700 nodes and 11092 triangular elements for the entire mesh. The smallest discretization in the horizontal direction is 0.5 μm while that in the vertical direction is 1 μm, and these are found around the three-electrode structure. This discretization was chosen to give sufficient accuracy in the calculation of the potential barrier field distribution.

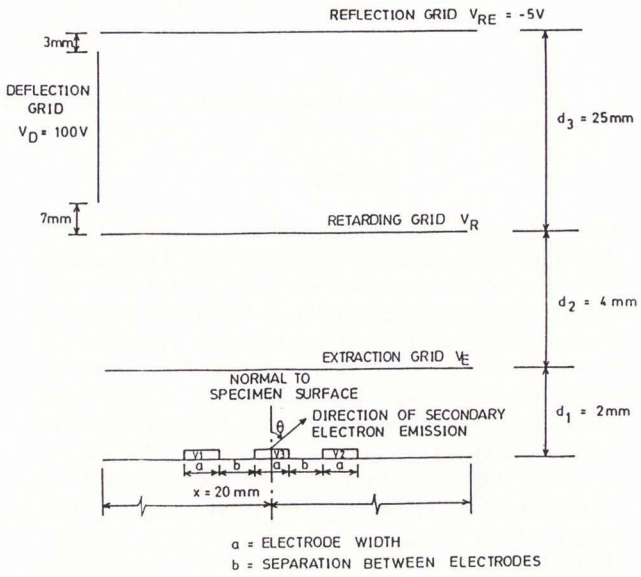

Fig. 1: Model of the planar retarding field energy analyser used in the theoretical study. Dimensions: a = b = 5 μm

A smaller simulation model having a width and height of 2mm by 2mm and confined to the area around the integrated circuit electrodes, was used to assess the effect of the potential barrier alone. The reduced dimensions of this second model allowed for a more accurate calculation of the potential barrier as this barrier exists only up to a few tens of microns above the surface.

Calculation of Potential Field Distribution

The potential distribution inside the specimen chamber of the SEM can be modelled by a Poissonian field. Since sources of charge generation are essentially negligible in the specimen chamber, the problem reduces to that of the simpler Laplacian field distribution.

The potential field distribution (φ) in the simulation model of an energy analyser inside the SEM specimen chamber is solved for the appropriate boundary conditions using a finite element program [2]. In the finite element solution of a partial differential equation, a geometrically complex domain is represented as a collection of geometrically simpler subdomains called finite elements. The differential equation of interest, i.e. Laplace equation in a two-dimensional space in this case, is expressed in an equivalent variational form. The solution of each element is assumed to be a combination of interpolation functions, L_i, i.e. $\varphi = L_i\varphi_i$. The parameters, φ_i, represent the values of the solu-

tion at a finite number of pre-selected nodes on the boundary and in the interior of the element.

A mesh generation program is used to discretize the simulation model into triangular finite elements. Triangular elements are chosen because they are the simplest polygonal figures into which a two-dimensional region can be subdivided. These elements can also be readily adapted to model irregular boundaries.

Electron Trajectory and S-Curve Computation

A trajectory tracking algorithm described in reference [2] is used to compute the SE trajectories. This algorithm assumes that the electric field varies linearly with distance within each mesh and was found to produce more accurate results than the "constant electric field within a fixed time step" approach, especially for low electron energies [2]. The SE current measured by the detector for each SE energy W is calculated as follows:

$$I(W) = N(W) \int \cos \Theta \, d\Theta \qquad (1a)$$

$$N(W) = 1.5 \, W \exp[2 - (8W/3)^{1/2}] \qquad (1b)$$

where the integration is computed for the angles of SE emission Θ which result in collection by the SE detector. (Θ is measured from the normal to the specimen surface in a clockwise direction.)

The simulation is carried out for angles of SE emission in discrete steps of 1^{o}. Changing the variable from Θ to α, (where α is the angle of SE emission measured from the horizontal in a counter-clockwise direction), the discrete form of eqn. (1a) is obtained as follows:

$$I(W) = N(W) \, \Sigma \cos (90^{o} - \alpha_i) \qquad (2)$$

α_i = Angle of collected SEs

The normalised total SE current calculated for a particular value of (VS - VR) is given by:

$$I_{nor} = I / I_{max} \qquad (3)$$

$$\text{where } I = \int_{W=0eV}^{50eV} I(W) \, dW \qquad (4)$$

$$I_{max} = [\sum_{\alpha_n=0^{o}}^{180^{o}} \cos (90^{o} - \alpha_n)] \int_{W=0eV}^{50 \, eV} N(W) \, dW \qquad (5)$$

A plot of the normalised SE current, I_{nor} in eqn. (3), versus (VS - VR) is known as the modified S-curve. The choice of the integration limits in eqn. (4) arises from the definition of SEs as electrons possessing energies in the range of 0 to 50 eV. The error voltages are calculated by noting the relative shift, δ(VS - VR), between two respective modified S-curves as explained below in the subsequent sections.

Isolation of Error Components

The large simulation model is used to compute the error voltage arising from the combined influence of the following:

a) Potential barrier and off-normal incidence injection effects, and
b) Potential barrier, off-normal incidence injection and analyser geometry effects.

To neutralise the influence of the analyser geometry effect in (a), the model is treated as an analyser of infinite width. Secondary electrons hitting the sides of the analyser before reaching the retarding grid plane will have their trajectories extrapolated to this plane if they have sufficient energy to overcome the uniform retarding field. The error voltage component due entirely to analyser geometry effect alone is isolated by subtracting the error voltages computed in part (b) from that of part (a) above.

To isolate the error voltage component due to the potential barrier effect from that of the off-normal incidence injection effect, the smaller simulation model of dimensions 2 mm by 2 mm is used [1]. In this smaller model, collection is assumed if a SE has sufficient energy to overcome this barrier. The error voltage resulting from this computation will be due to the potential barrier effect only. This component when subtracted from the error voltage due to the combined influence of the potential barrier and the off-normal incidence injection effects will give the error voltage component due to the latter effect alone.

TABLE 1: Summary of simulation models used for computing error voltage components.

Discretization Scheme	**Effects taken into into account for Error Voltage Computation**
SIMULATION MODEL: 20mm by 31mm Mesh	
Horiz axis: 95 points Vert axis : 60 points No. of Nodes : 5700 No. of Elements: 11092	1) Potential Barrier & Off-normal Injection Effects
	2) Potential Barrier, Off-normal Injection & Analyser Geometry Effects
SIMULATION MODEL: 2mm by 2mm Mesh	
Horiz axis: 113 points Vert axis : 58 points No. of Nodes : 6554 No. of Elements: 12768	Potential Barrier Effects Only

The two simulation models described above are summarised in Table 1. The individual error voltage components due to all three effects can be isolated from the computational results using these two models.

Simulation Results and Discussion

Type I Local Field Effect (LFE)

(a) Positive Specimen Voltage Type I LFE, or the effect of the finite size and voltage of the specimen electrode, is simulated by setting VS = 5 V and V1 = V2 = 0 V in fig. 1. Linearization error voltages arising from type I LFE are obtained by calculating the difference, δ(VS - VR), between the modified S-curves for (V1,VS,V2) = (0,5,0) V and (0,0,0) V. The effects of the potential barrier, off-normal incidence injection into the retarding field and the analyser geometry are each considered in turn and the error voltage component due to each individual effect is then calculated as described previously.

In figs. 2 to 5, the case where only the potential barrier effect is present is denoted by PBE. OFF-INC represents the situation where both the potential barrier effect and the off-normal incidence injection effect of SEs into the retarding field are present, while OFF-INC/GDE takes into account the analyser geometry effect in addition to the above-mentioned two effects.

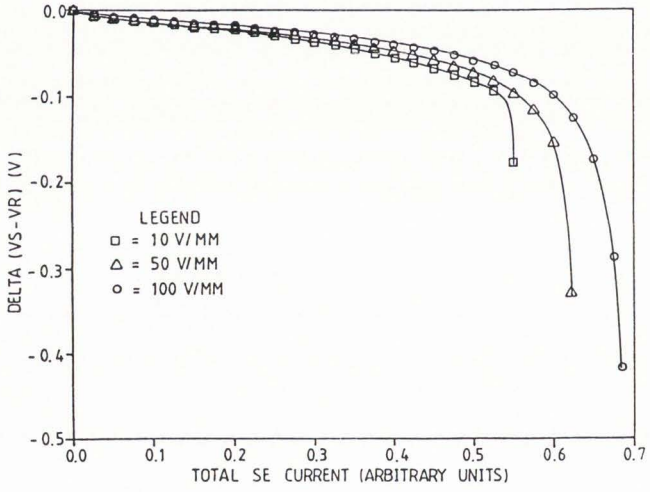

Fig. 2: Linearisation error voltages at extraction voltages of 10 V/mm, 50 V/mm and 100 V/mm, computed considering only the potential barrier effect. VS is set at 5 V.

Fig. 2 shows the linearization error voltage component due to the potential barrier effect alone for the case of (V1,VS,V2) = (0,5,0) V and three different extraction fields of 10 V/mm, 50 V/mm and 100 V/mm. A higher extraction field gives rise to a smaller error voltage as a result of a smaller potential barrier. The potential barriers for the above three extraction fields of 10, 50 and 100 V/mm are 4.22 V, 3.27 V and 2.55 V respectively. All the linearization error voltages are negative in this case which means that the total SE current for VS = 5 V is less than that of VS = 0 V (See Table 2 for summary of results at a normalised SE current of 0.5 units).

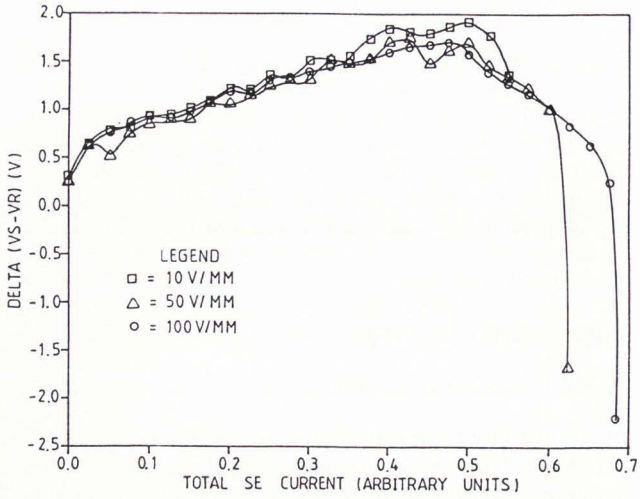

Fig. 3: Linearisation error voltages at extraction voltages of 10 V/mm, 50 V/mm and 100 V/mm, computed considering only the potential barrier and off-incidence injection effects. VS is set at 5 V.

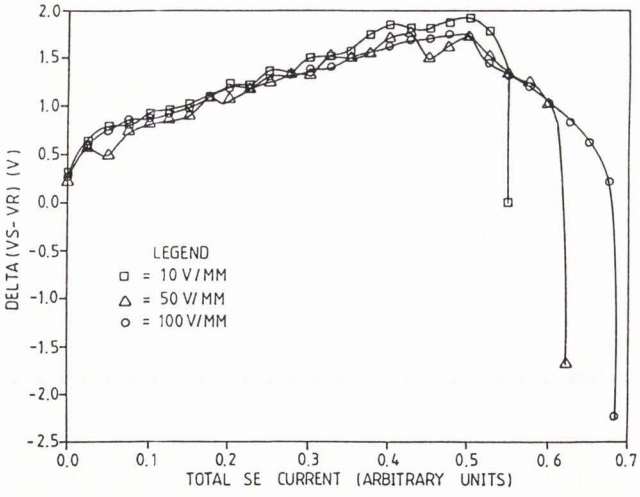

Fig. 4: Linearisation error voltages at extraction voltages of 10 V/mm, 50 V/mm and 100 V/mm, computed considering the potential barrier, off-incidence injection effects and analyser geometry dependent effects. VS is set at 5 V.

Table 2: Linearization (or Type I LFE) error voltages contributed by the potential barrier effect alone at a normalised SE current of 0.5 units and a 5 V specimen bias for three different extraction fields of 10, 50 and 100 V/mm.

Extraction Field (V/mm)	Potential Barrier (V)	Linearization Error Voltage (V)
10	4.22	-0.083
50	3.27	-0.072
100	2.55	-0.057

Fig. 3 shows the linearization error voltage when both the potential barrier effect and the off-normal incidence injection effect of SEs into the retarding field are taken into consideration. The plot in Fig. 4 takes into account the analyser geometry effect in addition to the two effects in Fig. 3. From these figures, it can be seen that the off-normal incidence injection effect of SEs accounts for the bulk of the linearization error voltage in type I LFE. This is much clearer when the three situations of PBE, OFF-INC and OFF-INC/GDE are plotted together in the same figure for each extraction voltage. This is shown in Figs. 5a, b and c for the extraction voltages of 10, 50 and 100 V/mm respectively. Table 3 summarizes the linearization error voltage contributed by both the potential barrier and off-normal incidence injection effects for three different extraction fields at a normalised SE current of 0.5 units, while Table 4 is a summary under similar conditions with the addition of the analyser geometry effect.

The error voltage component due to each individual effect can be isolated by subtracting the appropriate linearization error voltage curves, assuming no interaction occurs between the individual effects. For example, the error voltage component due to the off-normal incidence injection effect of SEs is obtained by subtracting the appropriate curve in Fig. 3 from the corresponding one in Fig. 2, or the appropriate value in Table 3 from the corresponding one in Table 2. The result is shown in Table 5 with respect to a normalised SE current of 0.5 units for all three extraction fields. Once again, it can be seen that the off-normal incidence injection effect of SEs account for a substantial portion of the error voltage.

The linearization error voltage decreases by only 11% and 17% for a 5 and 10 times respective increase in the extraction field from 10 V/mm. This shows that the relationship between the increase in the extraction field and the decrease in the linearization error voltage does not bear a simple linear relationship. This has also been reported in our previous paper for the case of very narrow energy analysers or in situations where the measurement point on the specimen is very near to the edge of the analyser [1].

Unlike the situation in reference [1] however, the analyser here is 20mm wide and the specimen measurement point is at the centre of the analyser. The extraction field and the Type I LFE concentrates the majority of the extracted SEs within a

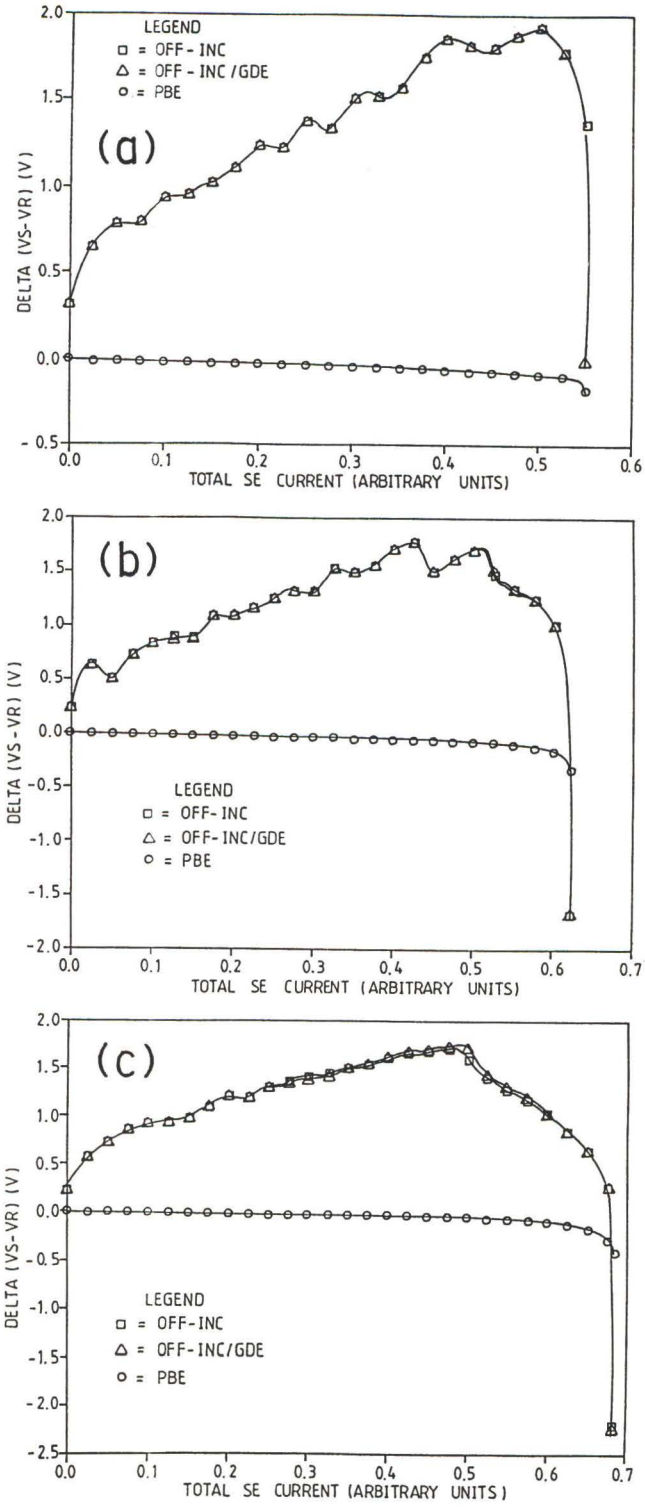

Fig. 5: Linearisation error voltages computed considering only potential barrier effect (PBE), potential barrier effect plus off-incidence injection effects (OFF-INC), potential barrier effect plus off-incidence injection effect and geometry dependent effect (OFF-INC/GDE), for extraction voltages of (a) 10 V/mm, (b) 50 V/mm and (c) 100 V/mm. VS is set at 5 V.

Table 3: Linearization (or Type I LFE) error voltages contributed by both potential barrier effect and off-normal incidence injection effect of SEs. The error voltages shown are at a normalised SE current of 0.5 units and a 5 V specimen bias for three different extraction fields of 10, 50 and 100 V/mm.

Extraction Field (V/mm)	Linearization Error Voltage (V)
10	1.933
50	1.712
100	1.606

Table 4: Linearization (or Type I LFE) error voltages contributed by the combined effects of the potential barrier, off-normal incidence injection of SEs and analyser geometry (20 mm wide energy analyser). The error voltages shown are at a normalised SE current of 0.5 units and a 5 V specimen bias for three different extraction fields of 10, 50 and 100 V/mm.

Extraction Field (V/mm)	Linearization Error Voltage (V)
10	1.930
50	1.720
100	1.733

cone of $\pm$ 2mm from the point of emission and well away from the analyser edges, resulting in an almost negligible error voltage component due to analyser geometry (see Table 5). This concentration of the trajectories is illustrated in Figs. 6a and 6b which show the extracted SE trajectories (in steps of 10^{o} emission angle) for SE energies of 6 eV and 8 eV respectively. These figures were obtained with a specimen bias of 5 V under a 10 V/mm extraction field. The horizontal extent of the plots is 2 mm in both figures. The increase in the error voltage due to the analyser geometry effect for the 100 V/mm field in Table 5 can be explained by the small errors incurred in the SE trajectory computation during cross-over between adjacent meshes. These errors can be reduced by increasing the number of iteration steps during mesh transitions.

The above results show that a substantial portion of the linearization error on a 20 mm wide analyser, whose measurement point is at or near the centre of the analyser, can be attributed to the off-normal incidence injection effect of SEs emitted into the retarding field. Even for a moderately strong extraction field of 100 V/mm, the error contribution of this effect could be as high as 30% to 40% of the voltage being measured. Conventional planar retarding field energy analysers suffer from this shortcoming as they measure only the longitudinal velocity of the SE instead of its total energy.

Table 5: Components of linearization (or Type I LFE) error voltage contributed by each individual effect at a normalised SE current of 0.5 units for three different extraction fields of 10, 50 and 100 V/mm. The SE emission point is at the centre of the specimen electrode and all error voltage components shown are for a 5 V specimen bias with the neighbouring electrode voltages set to zero.

Effect	Linearization Error Voltage Component (V)		
	10 V/mm	50 V/mm	100 V/mm
Potential Barrier Effect	-0.083	-0.072	-0.057
Off-normal Injection of SEs into retarding field	2.016	1.784	1.663
Analyser Geometry Effect (20 mm wide energy analyser)	-0.003	0.008	0.127

This effect must be taken into consideration during the design of energy analysers if the accuracy of quantitative voltage contrast measurements are to improve. There are several approaches taken to minimise this effect. One is to make use of hemispherical grids in energy analyser designs so that the SEs are essentially injected at near normal incidence into the retarding or analysing field [16,17,11]. A more recent approach is to make use of a collimating magnetic field to parallelize the SE trajectories before energy filtering so that the SEs enter the analysing field at near normal incidences [7,9,15].

(b) Negative Specimen Voltage The modified S-curve for a negative specimen bias VS of -5 V (Neighbouring electrode voltages V1 = V2 = 0 V) under a 100 V/mm extraction field in which all three effects (i.e. potential barrier, off-normal incidence injection and analyser geometry) are present is plotted in Fig. 7 and compared to that of VS = 5 V and 0 V (V1 = V2 = 0 V in both cases). There is an absence of a saturation plateau in the S-curve of a negative VS because of the absence of a potential barrier directly above a negatively biased conductor track. However, the normalised SE current for the negative VS of -5V quickly falls below that of the positive VS. It is also noted that the detected SE current for a positive VS is greater than that for VS = 0 V which in turn is greater than that for a negative VS. This is explained by the focussing effect of the surrounding voltage V1 and V2 on the SE trajectories when the specimen voltage is positive as compared to a defocussing effect when the specimen bias is negative.

The linearization error voltage curve for VS = -5 V is calculated by taking the difference between the modified S-curves for (V1,VS,V2) = (0,-5,0) V and (0,0,0) V. This is plotted and compared to the linearization error voltage curve of VS = 5 V (the latter curve being obtained in the previous section) in Fig. 8. It is noted that the magnitude of the linearization error voltage for both negative and positive specimen voltages were approximately the same; that of the negative bias being slightly less for a particular SE current. The smaller error voltage for a negative VS is probably due to the absence of the potential barrier effect.

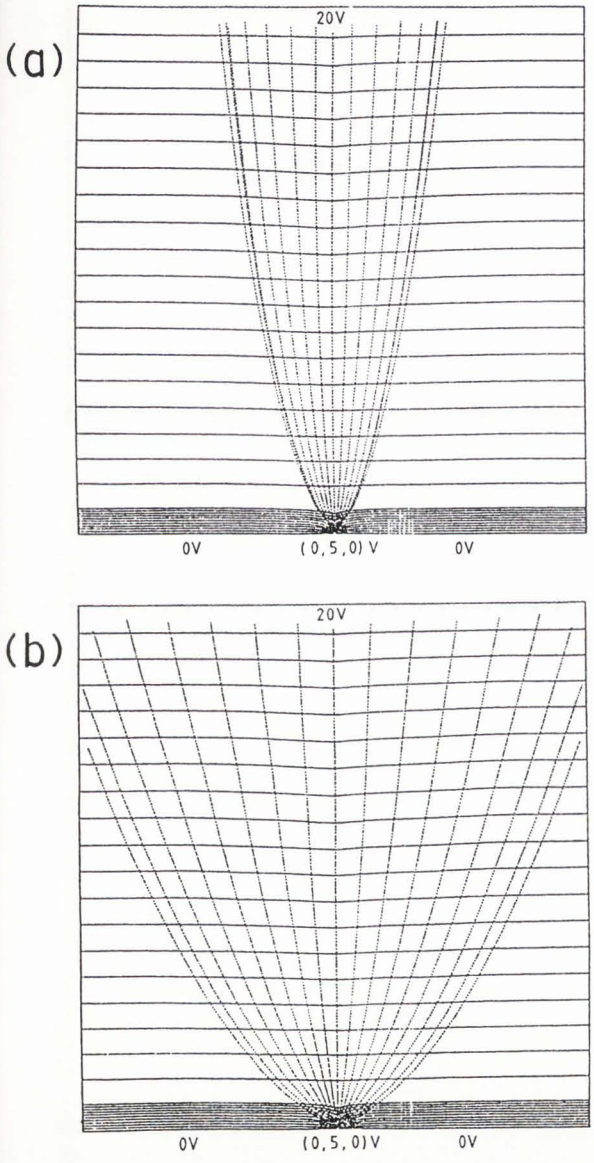

Fig. 6: Trajectories from secondary electrons (SE) emitted from a central conductor at 5V with neighbouring tracks set at 0V in an extraction field of 10 V/mm. The total width of the plot is 2 mm. In Fig. 6 (a), the SE energy is 6 eV while in Fig. 6(b) the SE energy is 8 eV.

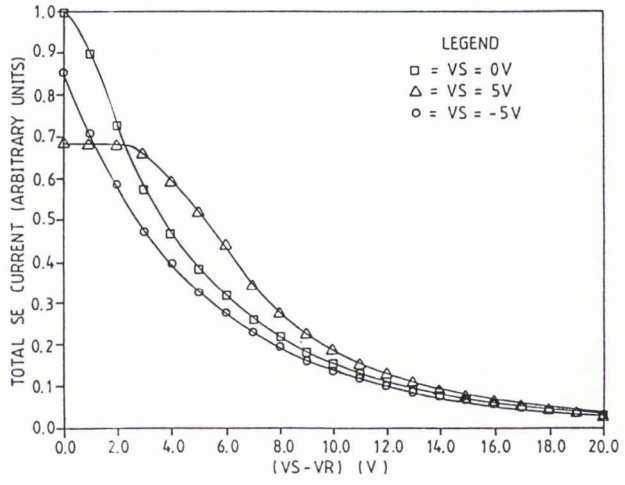

Fig. 7: S-curves computed by considering all three effects (OFF-INC/GDE) for VS of 5 V, 0 V and -5 V. Extraction field is 100 V/mm and neighbouring voltages, V1 and V2 is zero.

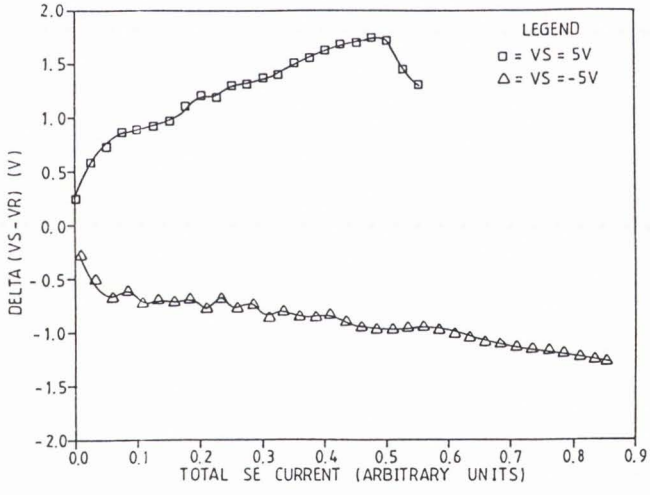

Fig. 8: Total linearisation (Type I local field) error voltages for VS at 5V and VS at -5V. All three effects are taken into account. Extraction field is 100 V/mm.

However, the off-normal incidence injection effect, owing to the influence of the type I local fields on the SE flight direction, will still be present and contribute a larger component to the total linearization error voltage. This is because, with V1 and V2 at zero voltage, a negative specimen bias VS tends to have a defocussing or deparallelizing effect on the SE trajectories unlike a positive specimen bias which has a focussing effect.

Type II Local Field Effect (LFE)

In quantitative voltage contrast, type II LFE, or the effect of the voltages of neighbouring electrodes, gives rise to a measurement error known as false voltage. Type II LFE is simulated by setting one of the neighbouring electrode voltages to a non-zero value, in this case V2. This is performed under a 100 V/mm extraction field for two values of V2 of 5 V and -5 V and for specimen biases VS of 0 V and 5 V. The computed modified S-curves and false voltage curves are shown in Figs. 9 and 10 respectively. The false voltages in Fig. 10 are obtained as follows:

a) For VS=0V, V2=5V: By calculating the difference δ(VS - VR) between the (V1, VS, V2) = (0,0,5) V and (0,0,0) V modified S-curves.

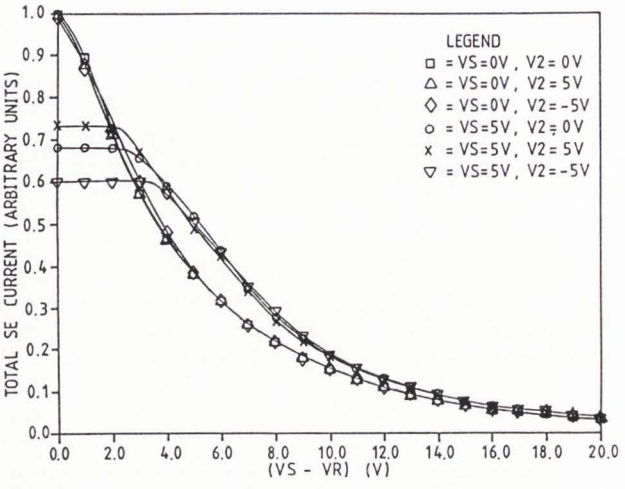

Fig. 9: S-curves for different specimen bias conditions. All three effects are taken into account. Differences in S-curves indicate presence of Type II local field effect. Extraction field is 100 V/mm.

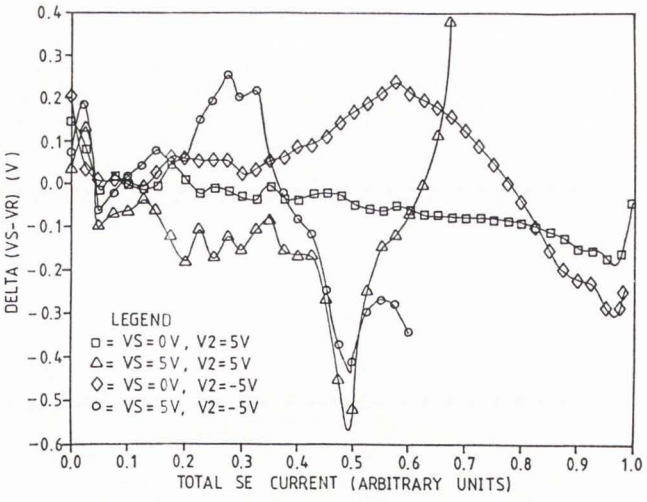

Fig. 10: Total false voltage arising from Type II local field errors at 100 V/mm for four conductor voltage combinations. All three effects are taken into account.

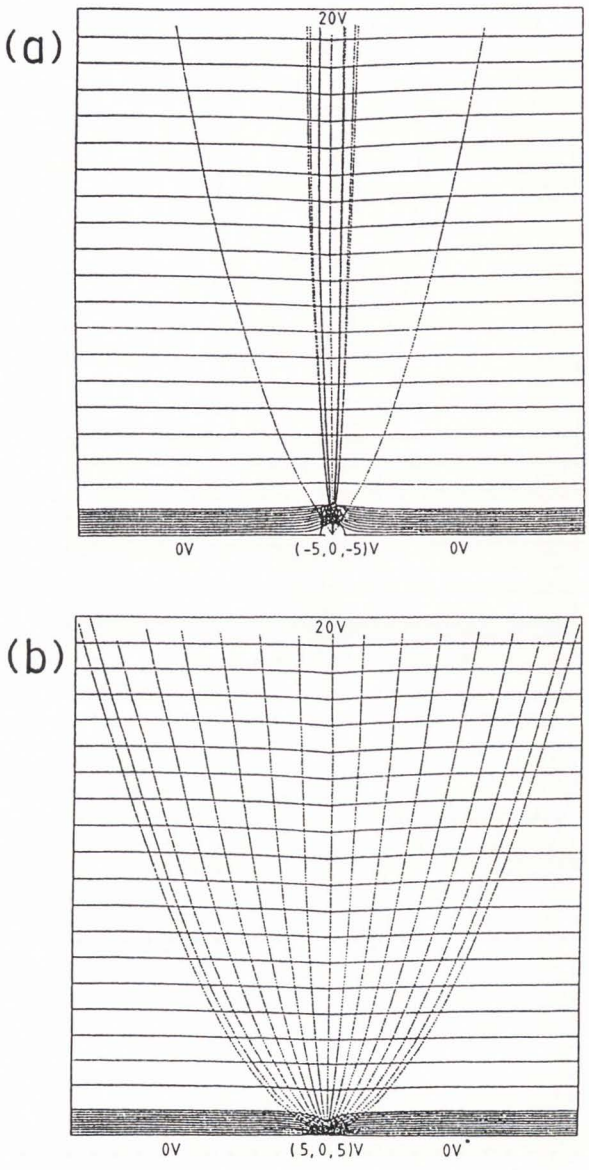

Fig. 11: Trajectories from 2 eV secondary electrons emitted from a central conductor with neighbouring tracks set at different voltages. The extraction field is 10 V/mm. The total width of the plot is 2 mm. In Fig. 11 (a), the specimen bias is (-5, 0, -5) V while in Fig. 11(b) the specimen bias is (5, 0, 5)V.

b) For VS=5V, V2=5V: By calculating the difference δ(VS - VR) between the (V1,VS,V2) = (0,5,5) V and (0,5,0) V modified S-curves.

c) For VS=0V, V2=-5V: By calculating the difference δ(VS - VR) between the (V1,VS,V2) = (0,0,-5) V and (0,0,0) V modified S-curves.

d) For VS=5V, V2=-5V: By calculating the difference δ(VS - VR) between the (V1,VS,V2) = (0,5,-5) V and (0,5,0) V modified S-curves.

It is observed from Fig. 10 that with the same V2, there is a much greater variation in the false voltage as a function of the total SE current for a non-zero, positive specimen bias VS than for a VS at 0 V. Fig. 10 also shows that the magnitude of the false voltage is about 3 to 10 times less than the linearization error voltage arising from type I LFE.

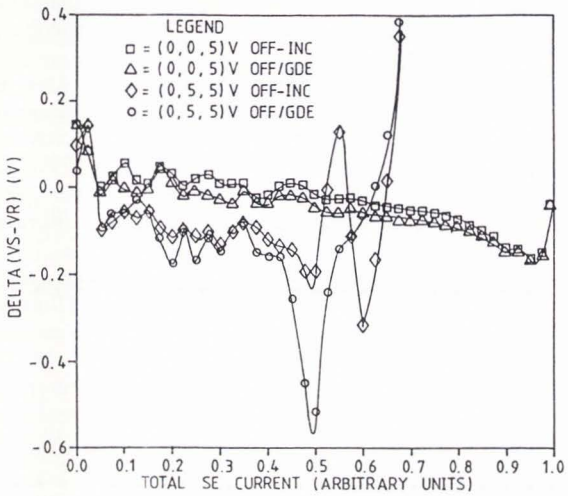

Fig. 12: Components of false voltages arising from Type II local field errors at 100 V/mm extraction field. OFF-INC represents the off-normal incidence effect alone; OFF/GDE represents the combination of off-normal incidence and geometry dependent effects.

The presence of a neighbouring electrode voltage has two main effects. The first effect concerns the potential barrier above the specimen electrode which is either raised or lowered depending on the polarity of the neighbouring electrode voltage; a positive V2 lowers the potential barrier while a negative V2 raises it. For a specimen bias VS of 5 V and a 10 V/mm extraction field, the potential barriers for V2 of -5 V, 0 V and 5 V are 4.54 V, 4.22 V and 3.96 V respectively. This accounts for the difference in the saturation plateau for the VS = 5 V modified S-curves in Fig. 9, a region of the curve which is primarily potential barrier limited. The second effect influences the SE trajectories; a positive V2 has a defocussing effect on the emitted SEs and this opposes the focussing effect of a positive VS. The focussing (defocussing) effect of a negative (positive) neighbouring electrode voltage is further illustrated in Figs. 11a and 11b, which are trajectory plots for (V1,VS,V2) = (-5,0,-5) V and (5,0,5) V respectively under a 10 V/mm extraction field and a 2 eV SE energy.

Fig. 12 shows the error voltage component curves for type II LFE with a neighbouring electrode voltage V2 of 5 V and a specimen bias VS of 0 V and 5V, denoted respectively by (V1,VS,V2) = (0,0,5) V and (0,5,5) V. All the plots are obtained under a 100 V/mm extraction field. OFF-INC represents the case where only the off-normal incidence injection of SEs into the retarding field is present, while OFF/GDE takes into account the analyser geometry effect in addition to the off-normal incidence injection effect.

It can be observed from Fig. 12 that the analyser geometry effect is relatively more significant compared to the off-normal incidence injection effect under type II LFE conditions than under type I LFE conditions. This is because the presence of a more positive neighbouring electrode tends to draw the SEs away from the central axis of the energy analyser, thus causing the electron trajectories to be more sensitive to the influence of analyser geometry. Overall, the error voltage component due to the analyser geometry effect is of the same order of magnitude as that due to the off-normal incidence injection effect. The type II error voltage or false voltage due to each individual effect is tabulated in Table 6 for a normalised SE current of 0.5 units.

Table 6: Type II LFE error voltage or false voltage components at a normalised SE current of 0.5 units under a 100 V/mm extraction field. The SE emission point is at the centre of the specimen electrode.

Effect	False Voltage Component (V) (0,0,5)V	(0,5,5)V
Off-normal Injection of SEs into retarding field	-0.0162	-0.195
Analyser Geometry Effect (20 mm wide energy analyser)	-0.0303	-0.334

Other Error Voltage Components

Although this study presents results of error voltage components for the above-mentioned three effects of potential barrier, off-normal incidence injection and analyser geometry, it is also recognised that other effects like lens effect, or the non-uniform field distribution across the gaps of analyser grids, could also contribute to an extra error voltage component. This area is presently under extensive study and results will be published at a later date.

Conclusion

Results of computer simulation investigations into the various error voltage components in quantitative voltage contrast are presented. In particular, the effects of the potential barrier, off-normal incidence injection of SEs into the analysing field and analyser geometry are quantified for a practical 20 mm wide planar retarding field energy analyser in situations where types I and II LFEs are present.

It is found that the error voltage component due to the off-normal incidence injection effect of SEs into the analysing field dominates the total linearization error due to type I LFE. Even for a moderately strong extraction field of 100 V/mm, the error contribution of this effect could be as high as 30% to 40% of the voltage being measured. The linearization error voltage due to a positive and negative specimen voltage is found to be approximately of the same magnitude.

As for type II LFE, there is a greater variation in the false voltage for a non-zero specimen bias than for a zero bias, the neighbouring electrode voltage being the same in both cases. Also, the magnitude of the false voltage is about 3 to 10 times less than the linearization error voltage arising from type I LFE. The false voltage component due to analyser geometry effect is of the same order of magnitude as that due to the off-normal incidence injection effect. The greater relative influence of analyser geometry effect under type II LFE conditions is due to the presence of a neighbouring electrode voltage which tends to draw the SEs away from the central axis of the energy analyser.

References

[1] Chan DSH, Low TS, Chim WK, Phang JCH (1988) The influence of analyser geometry effects in scanning electron microscope voltage contrast measurements. Scanning Microscopy 1988, 2, 1419-1426.

[2] Chim WK, Low TS, Chan DSH, Phang JCH (1988) Electron trajectory tracking algorithms for analysing voltage contrast signals in the scanning electron microscope. J. Phys. D: Appl. Phys. 21, 1-9.

[3] Chim WK, Phang JCH, Low TS, Chan DSH (1987) An overview of quantitative voltage contrast measurements in the scanning electron microscope. Proceedings of the 1st International Symposium on the Physical and Failure Analysis of Integrated Circuits, Singapore, 19-20 October 1987, 14-19, IEEE Singapore Section. (Available from IEEE Singapore, 200 Jalan Sultan, #11-03, Singapore 0719. Fax: 292-8596)

[4] De Jong JL, Reimer JD. (1986) Effects of local fields on electron beam voltage measurement accuracy. Scanning Electron Microsc. 1986; III: 933-942.

[5] Dinnis AR (1988), Detectors for Quantitative Electron Beam Voltage Measurements, Scanning Microsc., 2, 1407-1418.

[6] Fujioka H, Nakamae K, Ura K (1981) Local field effects on voltage measurement using a retarding field analyser in the scanning electron microscope. Scanning Electron Microsc. 1981; I: 323-332.

[7] Garth SCJ, Nixon WC, Spicer DF (1985) Accurate electron beam waveform measurement on high density integrated circuits. Microelectronic Engineering 3, 183-190.

[8] Khursheed A, Dinnis AR (1984) A Comparison of Voltage Contrast Detectors, Scanning, 6, 85-95.

[9] Kruit P, Dubbeldam L. (1987) An electron beam tester with dispersive secondary electron energy analyser. Scanning Microscopy 1, 1641-1646.

[10] Nakamae K, Fujioka H, Ura K (1981) Local field effects on voltage contrast in the scanning electron microscope. J. Phys. D: Appl. Phys., 14, 1939-1960.

[11] Nakamae K, Fujioka H, Ura K (1985) A new hemispherical retarding field energy analyser for quantitative voltage measurements in the SEM. J. Phys. E: Sci. Instrum. 18, 437-443.

[12] Nakamura H, Sato Y (1983) An analysis of the local field effect on electron probe voltage measurements. Scanning Electron Microsc. 1983; III: 1187-1195.

[13] Oatley CW and Everhart TE (1957) The examination of p-n junctions with the scanning electron microscope. J. Electron. 2, 568-570.

[14] Phang JCH, Koh PCT, Chin ISM, Ong KKW, Low TS and Chan DSH (1989) Integrated Circuit Fault Imaging with SEM Voltage Contrast. Proceedings of the 2nd International Symposium on the Physical & Failure Analysis of Integrated Circuits, 7-9 November 1989, pp21-26. (Available from IEEE Singapore, 200 Jalan Sultan, #11-03, Singapore 0719. Fax: 292-8596)

[15] Richardson N, Muray A (1987) An improved magnetic-collimating secondary electron energy filter for very large scale integrated diagnostics. J. Vac. Sci. Technol. B 6, 417-421.

[16] Tee WJ, Gopinath A. (1976) A voltage measurement scheme for the SEM using a hemispherical retarding analyser. Scanning Electron Microsc. 1976; IV: 595-602.

[17] Ura K, Fujioka H, Nakamae K (1984) Reduction of local field effect on voltage contrast. Scanning Electron Microsc. 1984; III: 1075-1080.

Discussion with Reviewers

AR Dinnis: Equation 1(a) is incorrect for the total SE emission. For the total emission into the sum of elemental rings extending for Φ from 0 to 2π and subtending an angle $d\Theta$, the expression should be:

$$I(W) = N(W) \int \sin(2\Theta)\, d\Theta$$

This is explained by L. Dubbeldam: "A voltage contrast detector with double channel energy analyser in a scanning electron microscope", PhD Thesis, Delft University Press, 1989, pp30-32.

Authors: The equation quoted by Dinnis describes total secondary electron emission in three dimensions. However, our simulation model is in two dimensions, and the potential distribution has been computed for two dimensions. The use of the suggested equation in this situation is therefore not appropriate because there is no circular symmetry in the Φ co-ordinate which the equation assumes. The application of our equation 1(a) results in a consistent two dimensional picture which corresponds to the signal from a line scan of the beam along a long centre electrode.

AR Dinnis: Can you explain the source of equation 1(b), the distribution of secondary electron energies? Is it to be preferred to the approximation of Chung and Everhart: "Simple calculation of low-energy secondary electrons emitted from metals under electron bombardment", J. Appl. Phys., 45, 707-709 (1974)?
A Gopinath: The exponential form of the energy distributions used to approximate the energy spread should be compared to other approximations for differences.
Authors: The energy distribution N(W) of SE from metals was measured by Kollath [Sekundarelektronen-Emission fester Korper bei Bestrahlung mit Electronen. Handbuch der Physik (Springer Berlin) Vol 21, 232-303 (1966)] and equation 1(b) is the fitted equation to his results. It gives very similar results to the Chung and Everhart expression.

A. Gopinath: The usual finite element approach is with linear variation of potential within the triangle. Have the authors used second order elements, and if so, what type of node distribution was used? Some details would be useful. How much better are the results with this new approach, and how do the authors' define better since the results are theoretical/numerical only?
Authors: No, we have not used second order elements as their benefits in these applications are not commensurate with the computational cost.

M. Schottler: Why do you only simulate electrodes with 5 μm dimensions, and do you think that the simulated errors will increase with decreasing electrode size and spacing?
Authors: This spacing was chosen to illustrate the effects. The same technique can be used for smaller electrode size and spacing and we would expect the errors to be more severe.

H. Fujioka: In your calculation, is the thickness of the specimen electrode taken into account?
Authors: No, the electrode was assumed to have insignificant height.

AR Dinnis: Have you considered the effect of magnetic fields deliberately or unintentionally introduced, on the performance of detectors?
Authors: Studies on magnetic extraction are being conducted at present.

AR Dinnis: Does the computation of surface fields include the effect of a layer of insulators between the conductors and the underlying silicon?
Authors: The computation assumes that the space between the electrodes is insulating. However, the computation does not take into account charging effects below the electrode plane.

A. Gopinath Is there no method of reducing the Type I error below the 30 to 40% predicted?
Authors: It would appear from our results that reducing the off-normal incidence injection of SEs into the retarding field will reduce Type I error significantly. This is further described in detail in the last paragraph of subsection (a) Positive Specimen Voltage in section Type I Local Field Effect in Siumulation Results and Discussion.

M. Schottler: Do you see a chance to verify the simulated results by measurements?
S. Utterback: Can you suggest a means of quantitatively measuring the effects you have treated theoretically? How can this information be used to correct for these effects?
H. Fujioka: Is it possible to separate the error voltage components due to potential barrier formation and off-normal incidence? Would you please explain in some more detail how you could calculate the error voltage component due to the potential barrier effect "alone"?
Authors: Verification of the simulation results is currently being carried out. A suggested means would be to measure the errors with a hemispherical detector, a very wide planar detector and a narrow planar detector. Comparison of data from these three analysers will allow the separation of the error components. This information is probably more useful for designing analysers with minimum error components rather than for correcting measurements already made.

S. Utterback: In analysing the types of effects that can be expected to contribute the error in quantitative voltage contrast, the effect of the actual electric field distribution within the plane of the retarding grid is mentioned as a possible contributing factor but is not treated in any way. Presumably the effect of the grid mesh size on error components will arise principally due to changes in electron direction caused by local field inhomogeneities. (a) Please comment on the mechanism of the error contribution and make a general assessment of this effect. (b) Is it likely to dominate the effects already treated? (c) How can this effect be minimised (sample/grid geometry)?
Authors: The mechanism is due to the fields in the lateral direction in the extraction and retarding grid planes and possible interpenetration effects due to non-uniformity of potential on the retarding grid plane. The contribution of this mechanism to total error is presently being investigated. Preliminary studies show that the effects can be significant but can be controlled with careful design of the energy analyser.

A. Gopinath: Could the authors identify where their results are new or differ from previous work?
Authors: As far as we are aware, there are no published reports which quantify the contributions of the various error components in voltage contrast measurements. We believe this is useful data in the design of optimised energy analysers.